SCIENCE CHINA
Information Sciences

• **Supplementary File** •

Characteristic Model-based Control of Robotic Manipulators with Dynamic Uncertainties

Wang Lijiao[1] & Meng Bin[1*]

[1]*Science and Technology on Space Intelligent Control Laboratory, Beijing Institute of Control Engineering, Beijing* 100190, *China*

Appendix A Proof of Lemma 4

Since $\Delta\bar{\theta}_1(k) = G_{C0}(k)\left[G_{C0}(k)^{-1} - \hat{G}_{C0}(k)^{-1}\right]$, we have

$$\Delta\bar{\theta}_1(k) = I_n - G_{C0}(k)\hat{G}_{C0}(k)^{-1}$$

If $\hat{G}_{C0}(k) = \frac{1}{2}(b_1 + b_0)I_n$, we can derive from Lemma 1 and (13) that

$$\|\Delta\bar{\theta}_1(k)\| \leqslant \left\|I_n - \frac{2}{b_1 + b_0}G_{C0}(k)\right\| \leqslant \frac{b_1 - b_0}{b_1 + b_0}$$

Appendix B Proof of Lemma 5

Since $\Delta\bar{\theta}_2(k) = G_{C0}(k)\left[G_{C0}(k)^{-1}F_{C2}(k) - \hat{G}_{C0}(k)^{-1}\hat{F}_{C2}(k)\right]$, we have

$$\begin{aligned}\|\Delta\bar{\theta}_2(k)\| &= \|F_{C2}(k) - (I_n - \Delta\bar{\theta}_1(k))\hat{F}_{C2}(k)\| \\ &\leqslant \|\Delta\bar{\theta}_1(k)\|\|\hat{F}_{C2}(k)\| + \|(I_n + F_{C2}(k)) - (I_n + \hat{F}_{C2}(k))\|\end{aligned}$$

According to (13) and Lemma 2, we further derive

$$\|\hat{F}_{C2}(k)\| \leqslant 1 + \|I_n + \hat{F}_{C2}(k)\| \leqslant 1 + k_e\|e(k)\|$$

$$\|(I_n + \hat{F}_{C2}(k)) - (I_n + F_{C2}(k))\| \leqslant 2k_e\|e(k)\|$$

Then, by Lemma 4, we get

$$\|\Delta\bar{\theta}_2(k)\| \leqslant b_2 + b_3k_e\|e(k)\|$$

Appendix C Proof of Theorem 1

Before the stability analysis, we first analyze the feasibility of (16). By (15) and the expression of b_2 in Lemma 4, it is easy to obtain that $b_2 < \frac{\mu}{\mu+2}$. Thus, the right hand of (16) is positive, which means that there exists T_s such that (16) holds.

Next, we proceed to perform stability analysis for the closed loop, which can be divided into two parts, i.e., the kinematic module (7) and the dynamic module (14). We first analyze the property of the kinematic part (7), which can be rewritten as

$$q(k+1) = \epsilon q(k) + s(k+1)$$

Then, by iteration, we get

$$\|q(k)\| \leqslant \|q(0)\|\epsilon^k + \frac{1-\epsilon^k}{1-\epsilon}\max_{1\leqslant\bar{\tau}\leqslant k}\|s(\bar{\tau})\|, \quad k \geqslant 1 \tag{C1}$$

Since (16) ensures $T_s < 1$, we have $0 < \epsilon < 1$ and $0 \leqslant \frac{1-\epsilon^k}{1-\epsilon} < \infty$. Also, as $k \to \infty$, $\|q(0)\|\epsilon^k \to 0$. Obviously, the boundedness of $q(k)$ is ensured provided that $s(\bar{k})$ is bounded, $\forall \bar{k} \in \{1, \cdots, k\}$.

* Corresponding author (email: mengb@amss.ac.cn)

Then, we will employ the induction method to get the quality of $s(k)$, and the recursion formula of $\|s(k)\|$ should be derived beforehand. By (14), we have

$$\|s(k+1)\| \leqslant \|\Delta\bar{\theta}_2(k)\|\|s(k)\| + T_s\|\Delta\bar{\theta}_1(k)\|\|q(k)\| + T_s\|\Delta\bar{\theta}_2(k)\|\|q(k-1)\| \tag{C2}$$

Substituting $\|\Delta\bar{\theta}_1(k)\| \leqslant b_2$ and $\|\Delta\bar{\theta}_1(k)\| \leqslant b_2 + b_3k_e\|e(k)\|$ into (C2) yields

$$\|s(k+1)\| \leqslant (b_2 + b_3k_e\|e(k)\|)\|s(k)\| + T_sb_2\|q(k)\| + T_s(b_2 + b_3k_e\|e(k)\|)\|q(k-1)\| \tag{C3}$$

Since $e(k) = q(k) - q(k-1)$, we get from (7) that

$$\|e(k)\| \leqslant \|s(k)\| + T_s\|q(k-1)\| \tag{C4}$$

Substituting (C1) and (C4) into (C3), we get

$$\begin{aligned}\|s(k+1)\| \ \leqslant\ & \delta_0(k)\|s(k)\| + \delta_1(k)\|s(k)\|^2 + \delta_2(k)\|s(k)\|\max_{1\leqslant\bar{\tau}\leqslant k-1}\|s(\bar{\tau})\| \\ & + \delta_3(k)\max_{1\leqslant\bar{\tau}\leqslant k}\|s(\bar{\tau})\| + \delta_4(k)\max_{1\leqslant\bar{\tau}\leqslant k-1}\|s(\bar{\tau})\| \\ & + \delta_1(k)\left(\max_{1\leqslant\bar{\tau}\leqslant k-1}\|s(\bar{\tau})\|\right)^2 + \delta_5(k)\bar{s}, \quad \forall k \geqslant 2\end{aligned} \tag{C5}$$

where $\delta_0(k) = b_2 + 2b_3k_eT_s\|q(0)\|\epsilon^{k-1}$, $\delta_1(k) = b_3k_e$, $\delta_2(k) = 2b_3k_e(1-\epsilon^{k-1})$, $\delta_3(k) = b_2(1-\epsilon^k)$, $\delta_4(k) = b_2(1-\epsilon^{k-1}) + 2b_3k_eT_s\|q(0)\|\bar{\epsilon}^{k-1}$, $\delta_5(k) = b_2(\epsilon+1)\epsilon^{k-1} + b_3k_eT_s\|q(0)\|\epsilon^{2(k-1)}$, $\epsilon = 1 - T_s$, and $\bar{s} = T_s(\|v(0)\| + \|q(0)\|)$.

Now, we proceed to give the quality of $s(k)$ by the induction method. When $k = 0$, we have $e(0) = q(0) - q(-1) = T_sv(0)$. Since $T_s < 1$, we get from (7) that

$$\begin{aligned}\|s(0)\| &= \|T_sv(0) + T_sq(-1)\| \\ &= \|T_s(1-T_s)v(0) + T_sq(0)\| \\ &\leqslant T_s(1-T_s)\|v(0)\| + T_s\|q(0)\| \\ &\leqslant \bar{s}\end{aligned}$$

By (14), we get

$$s(1) = -\Delta\bar{\theta}_2(0)T_sv(0) + T_s\Delta\bar{\theta}_1(0)q(0)$$

which further yields

$$\begin{aligned}\|s(1)\| &\leqslant T_s\|\Delta\bar{\theta}_2(0)\|\|v(0)\| + T_s\|\Delta\bar{\theta}_1(0)\|\|q(0)\| \\ &\leqslant T_s[b_2 + b_3k_eT_s\|v(0)\|]\|v(0)\| + T_sb_2\|q(0)\| \\ &\leqslant [b_2 + b_3k_e\bar{s}]\bar{s}\end{aligned}$$

Since (16) holds, we obtain

$$\|s(1)\| \leqslant \mu\bar{s} \tag{C6}$$

When $k = 1$, utilizing (C1), (C3) and (C4), we derive

$$\|s(2)\| \leqslant [(\mu+2)b_2 + \mu T_sb_2 + (\mu+1)^2b_3k_e\bar{s}]\bar{s}$$

Similarly, by use of (16), $\|s(2)\|$ satisfies

$$\|s(2)\| \leqslant \mu\bar{s}$$

Now, let us consider the case when $k \geqslant 2$ based on (C5) via the induction method. Assume $\forall\bar{k} = 1, \cdots, k_1$, $k_1 \geqslant 2$, $\|s(\bar{k})\| \leqslant \mu\bar{s}$ holds. Thus, (C5) can be reformulated as

$$\|s(k_1+1)\| \leqslant [\psi_1(k) + \psi_2(k)]\bar{s} \leqslant [(\mu+2)b_2 + (2\mu+1)^2b_3k_e\bar{s}]\bar{s} \tag{C7}$$

where

$$\begin{aligned}\psi_1(k) &= \mu[\delta_0(k) + \delta_3(k) + \delta_4(k)] + \delta_5(k) \\ \psi_2(k) &= \mu^2[2\delta_1(k) + \delta_2(k)]\bar{s}\end{aligned}$$

Then, by (16), we get

$$\|s(k_1+1)\| \leqslant \mu\bar{s}$$

As a result, we obtain by the induction method that

$$\|s(k)\| \leqslant \mu\bar{s}, \quad \forall k \geqslant 1 \tag{C8}$$

Now, we continue to show the property of $q(k)$. Substituting (C8) into (C1) gives rise to

$$\|q(k)\| \leqslant \|q(1)\|\epsilon^{k-1} + \frac{(1-\epsilon^k)}{T_s}\mu\bar{s}, \quad k \geqslant 1 \tag{C9}$$

By (C1) and (C6), we have

$$\|q(1)\| \leqslant \|s(1)\| + \epsilon\|q(0)\| \leqslant \|q(0)\| + T_s\|v(0)\| \tag{C10}$$

Substituting (C10) into (C9), we get

$$\|q(k)\| \ \leqslant\ \left((1-\mu\epsilon)\epsilon^{k-1} + \mu\right)\|q(0)\| + \left((T_s - \mu\epsilon)\epsilon^{k-1} + \mu\right)\|v(0)\|, \quad k \geqslant 1 \tag{C11}$$

This yields

$$\|q(k)\| \leqslant \begin{cases} (1+\mu T_s)\|q(0)\| + (T_s + T_s\mu)\|v(0)\|, & \text{when } T_s - \mu\epsilon \geqslant 0 \\ (1+\mu T_s)\|q(0)\| + \mu\|v(0)\|, & \text{when } T_s - \mu\epsilon < 0 \end{cases}$$

Let $c^* = \max\Big\{T_s(1+\mu), \mu\Big\}$. Then, $q(k)$ satisfies

$$\|q(k)\| \leqslant (1+\mu T_s)\|q(0)\| + c^*\|v(0)\| \tag{C12}$$

Obviously, $q(k)$ is UUB. By (C4), (C8) and (C12), it is easy to get

$$\|e(k)\| \leqslant T_s(\mu + 1 + T_s\mu)\|q(0)\| + T_s(\mu + c^*)\|v(0)\|, \quad \forall k \geqslant 1 \tag{C13}$$

Therefore, $e(k)$ is guaranteed to be bounded. Meanwhile, we derive from (C11) that

$$\lim_{k\to\infty} \|q(k)\| \leqslant \mu[\|q(0)\| + \|v(0)\|]$$

Appendix D Proof of Theorem 2

By (18) and (19), we get that (15) holds. Since T_s satisfies (16), the result in Theorem 1 is derived. According to (17), if we select a positive constant

$$\varepsilon = \frac{1-b_2}{2+b_2}[\|q(0)\| + \|v(0)\|] \tag{D1}$$

then there always exists a $k_T > 0$ such that

$$\|q(k)\| \leqslant \mu[\|q(0)\| + \|v(0)\|] + \varepsilon, \quad \forall k \geqslant k_T \tag{D2}$$

Substituting (D2) into (C4) and utilizing (C8), we have

$$\|e(k)\| \leqslant 2T_s\mu[\|q(0)\| + \|v(0)\| + \varepsilon], \quad k \geqslant k_T + 1$$

Then, we get from Lemma 4 that

$$\|\Delta\bar{\theta}_2(k)\| \leqslant b_2 + 2b_3k_eT_s\mu[\|q(0)\| + \|v(0)\| + \varepsilon], \ k \geqslant k_T + 1 \tag{D3}$$

Substituting (9) into (2) and employing Lemma 3, we get the closed-loop dynamics

$$q(k+1) = [(1-T_s)I_n - \Delta\bar{\theta}_2(k) + T_s\Delta\bar{\theta}_1(k)]q(k) + \Delta\bar{\theta}_2(k)q(k-1) \tag{D4}$$

Utilizing $\|\Delta\bar{\theta}_1(k)\| \leqslant b_2$, (D2) and (D3), we further derive

$$\|q(k+1)\| \leqslant a_1\|q(k)\| + a_2\|q(k-1)\|, \quad \forall k \geqslant k_T + 1 \tag{D5}$$

where $a_1 = 1 - T_s + b_2 + 2b_3k_eT_s\mu(\|q(0)\| + \|v(0)\| + \varepsilon) + T_sb_2$, $a_2 = [b_2 + 2b_3k_eT_s\mu(\|q(0)\| + \|v(0)\| + \varepsilon)]$. It is easy to obtain from (18), (19) and (D1) that

$$a_1 + a_2 < 1, \quad a_2 < 1 \tag{D6}$$

Rewrite (D5) in the state-space form, i.e.

$$X(k+1) \leqslant A_X X(k) \tag{D7}$$

where $X(k) = [\|q(k-1)\| \quad \|q(k)\|]^{\mathrm{T}}$ and $A_X = \begin{bmatrix} 0 & 1 \\ a_2 & a_1 \end{bmatrix}$. Obviously, all the eigenvalues of A_X are located inside the unit circle, indicating the spectral radius $\rho(A_X) < 1$. Therefore, there exist constants $0 < M_o < \infty$ and $0 < \lambda_o < 1$, such that $\|A_X^k\| \leqslant M_o\lambda_o^k$ [1]. Based on the results above, we construct an auxiliary system represented as

$$Y(k+1) = A_X Y(k), \ \ Y(k_T) = X(k_T) \tag{D8}$$

Since $a_1 > 0$, $a_2 > 0$, and all the elements of $X(k)$ are non-negative, we get

$$\|X(k)\| \leqslant \|Y(k)\|, \quad \forall k \geqslant k_T + 1 \tag{D9}$$

By (D8), we further get

$$\|Y(k)\| \leqslant \|A_X^k\|\|Y(0)\| \leqslant M_o\lambda_o^k\|Y(0)\| \tag{D10}$$

This implies that $\|Y(k)\|$ goes to 0 asymptotically. Then, from (D9) and (D10), the asymptotic convergence of $\|X(k)\|$ is derived, further leading to the result $\lim_{k\to\infty} q(k) \to 0$.

Appendix E Simulation

We validate the proposed characteristic model-based adaptive control scheme using a two-DOF planar robotic manipulator, as shown in Fig.E1. The physical parameters of the robot is

$$\bar{m}_1 = 1, \ l_1 = 1, \ r_1 = 1, \ \bar{m}_2 = 0.3, \ l_2 = 0.3, \ r_2 = 0.3$$

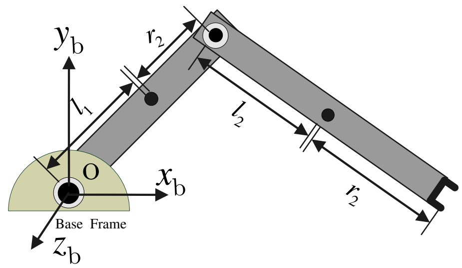

Figure E1 A 2-DOF planar robotic manipulator

where $\bar{m}_{\bar{i}}$, $l_{\bar{i}}$, $l_{\bar{i}}+r_{\bar{i}}$ denote the mass, the position of the center of mass, and the length of the $\bar{i}$th link, respectively, $\bar{i} \in \{1,2\}$. These physical parameters are unknown in controller design. The gravitational force is neglected in the simulation.

The initial joint position and velocity are respectively set as $q(0) = [\frac{1}{18}\pi,\ \frac{1}{10}\pi]^{\mathrm{T}}$, $v(0) = [0,\ 0]^{\mathrm{T}}$. The characteristic coefficients F_{C1}, F_{C2} and G_{C0} are uncertain due to the uncertainties of $\bar{m}_{\bar{i}}$, $l_{\bar{i}}$ and $l_{\bar{i}} + r_{\bar{i}}$, $\bar{i} \in 1, 2$. The projection based gradient estimation law (11)−(13) is adopted to estimate the characteristic coefficients online, where $B_0 = B_1 = 0.00145$, $k_e = 0.2$, $\lambda_1 = 0.8$ and $\lambda_2 = 1$. The initial characteristic model coefficients are set as $\hat{F}_{C1}(0) = 2I_2$, $\hat{F}_{C2}(0) = -I_2$, $\hat{G}_{C0}(0) = \frac{1}{2}(B_0 + B_1)I_2$. The controller bears the form (9).

To demonstrate the influence of T_s on the control performance, we make a comparison of different sampling periods in Fig.E2 and Fig.E3. Furthermore, disturbances with the amplitude $0.1 \times [1 + \sin(2\mathrm{t}), \cos(3\mathrm{t})]^{\mathrm{T}}$ are added to the position measurements to test the robustness of the strategy, and the controller is illustrated to be insensitive to disturbances, as shown in Fig.E4 and Fig.E5. The selection of the sampling time should take both the control performance and the stability into account. From the stability perspective, a smaller T_s is preferred to satisfy (16). However, the smaller T_s will lead to a larger control volume and make the system be more sensitive to noises owing to the difference term introduced by the controller. Meanwhile, the hardware constraint determines that T_s cannot be small enough. In practical applications, T_s can be selected by trial and error, as the traditional characteristic model-based control scenarios.

By simulation, we find that our controller bears strong robustness and the upper bound of T_s can be much more relaxed than the theoretical bound in (16). Compared with the discrete-time control protocols in [2–5], the characteristic model-based control strategy achieves satisfactory control performance with simpler control structure and less adjustable parameters.

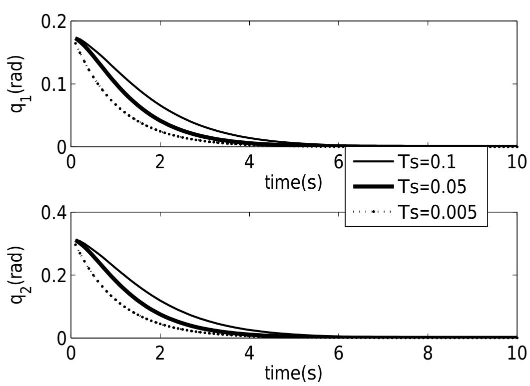

Figure E2 Joint-position response of the robotic manipulator

References

1 L. Guo. Time-varying stachastic systems-stability, estimation and control. Jilin Science and Technology Press, 1990

2 M. L. Corradini, V. Fossi, A. Giantomassi, G. Ippoliti, S. Longhi, G. Orlando. Discrete time sliding mode control of robotic manipulators: development and experimetal validation. Control Engineering Practice, 2012, 20, 816-822

3 Y. Yalcin, A. Astolfi. Immersion and invariance adaptive control for discrete-time systems in strick feedback form. Systems & Control Letters, 2012, 61, 1132-1137

4 F. Sun, H. Li, L. Li. Robot discrete adaptive control based on dynamic inversion using dynamical neural networks. Automatica, 2002, 38, 1977-1983

5 C. Treesatayapun. Discrete-time direct adaptive control for robotic systems based on model-free and if-then rules operation. International Journal of Advanced Manufacture Technology, 2013, 68, 575-590

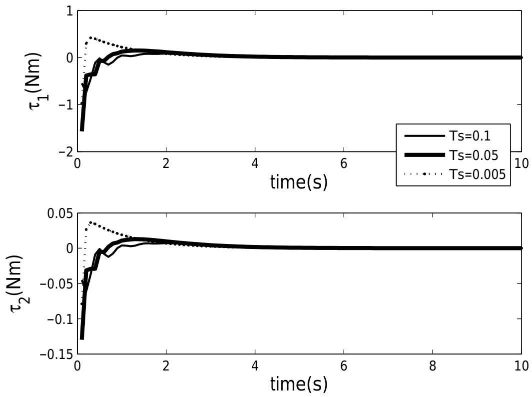

Figure E3 Control-torque response of the robotic manipulator

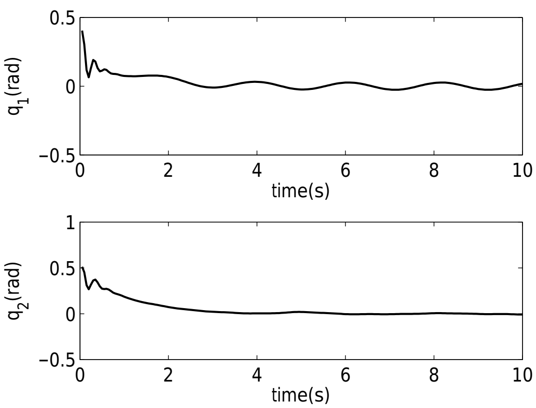

Figure E4 Position response with output disturbance (Ts=0.05s)

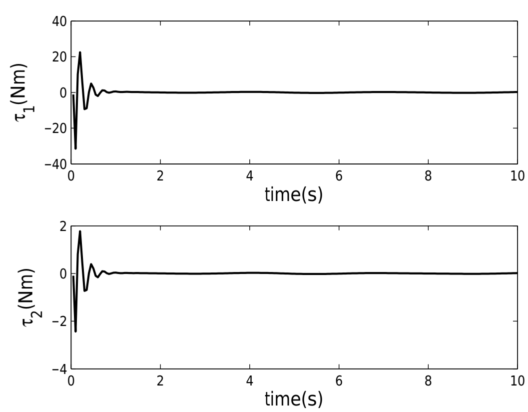

Figure E5 Control torque response with output disturbance (Ts=0.05s)